Cell Reports Medicine, Volume *5*

Supplemental information

The μ-opioid receptor differentiates two distinct human nociceptive populations relevant to clinical pain

Ellen S. Staedtler, Matthew R. Sapio, Diana M. King, Dragan Maric, Andre Ghetti, Andrew J. Mannes, and Michael J. Iadarola

Table S1. Efficacy of systemic opioids on human experimental heat pain, related to Figure 1, Introduction, and Discussion.

Author, year	Study specifics	Analgesic (dose & ROA)	Testing specifications	Effect on pain measures
Stacher et al. 1983[S1]	Double-blind, placebo-controlled	Meptazinol (100 mg, 200 mg, 400 mg po), Pentazocine (50 mg, 100 mg po)	Radiant heat on skin	No effect on pain detection thresholds for 100 mg Meptazinol, increase of pain detection thresholds for 200 mg and 400 mg Meptazinol and Pentazocine
Van Der Burgth et al. 1994[S2]	Double-blind, placebo-controlled	Morphine (0.15 mg/kg iv)	200 ms laser stimulation	No effect on warmth detection thresholds
Gustorff et al. 2003[S3]	Double-blind, active placebo-controlled	Remifentanil (0.08 µg/kg*min iv)	Contact heat on skin	Increase of pain detection thresholds and pain tolerance
Naef et al. 2003[S4]	Double-blind, (active) placebo-controlled	Morphine (30 mg po)	Contact heat on skin	No effect on pain detection thresholds and pain tolerance
Angst et al. 2004[S5]	Double-blind, (active) placebo-controlled, crossover	Alfentanil (20, 40, 80, and 160 ng/ml plasma concentrations iv)	Contact heat on skin	Increase of pain detection thresholds and pain tolerance
Cortinez et al. 2004[S6]	(active) placebo-controlled, crossover	Remifentanil (1-4 ng/ml plasma concentrations, iv)	Contact heat on skin	Decrease in pain ratings
Fillingim et al. 2005[S7]	Double-blind, placebo-controlled, crossover	Morphine (0.08 mg/kg iv)	Contact heat on skin	Increase of pain detection thresholds and pain tolerance, decrease of pain intensity ratings
Arendt-Nielsen et al. 2009[S8]	Double-blind, (active) placebo-controlled, crossover	Oxycodone (15 mg po)	Contact heat esophagus	Increase in pain detection thresholds
Eisenberg et al. 2010[S9]	Double-blind, active placebo controlled	Oxycodone (0.3mg/kg po)	Contact heat on skin	No effect on pain detection thresholds
Andresen et al. 2011[S10]	Double-blind, placebo-controlled, crossover	Fentanyl (25 µg/h, transdermal), Buprenorphine (20 µg/h, transdermal)	Contact heat on skin	No effect on pain tolerance (Fentanyl), increase of pain tolerance (Buprenorphine)
Angst et al. 2012[S11]	Double-blind, placebo-controlled	Alfentanil (100 ng/ml plasma concentration, iv)	Contact heat on skin	Increase of pain detection threshold

King et al. 2013[S12]	Double-blind, (active) placebo-controlled, crossover	Morphine (0.08mg/kg iv), Pentazocine (0.5 mg/kg iv)	Contact heat on skin	Increase of pain detection threshold and pain tolerance, decrease of pain intensity ratings for temporal summation trials (Morphine). No effect on pain detection thresholds, increase of pain tolerance, decrease of pain intensity ratings for temporal summation trials (Pentazocine).
Olesen et al. 2014[S13]	Double-blind, placebo-controlled, crossover	Morphine (30 mg po)	Contact heat on skin and rectal	No effect on pain tolerance (all testing locations)
Prosenz & Gustorff 2017[S14]	Double-blind, (active) placebo-controlled, crossover	Fentanyl (1 µg/kg iv)	Contact heat on skin	Decrease in pain ratings

These studies explored mostly noxious heat on superficial tissue (skin). Opioids show analgesic efficacy in the majority of studies, with more consistent effect on pain tolerance than pain thresholds. Given the nature of the majority of stimuli (heat ramp), pain thresholds are reached faster and at lower temperatures (more phasic stimulation) than pain tolerance (more sustained stimulation, reaching deeper skin layers).

Table S2. Efficacy of systemic opioids on human experimental cold pain, related to Figure 4, Figure S6, Introduction, and Discussion.

Author, year	**Study specifics**	**Analgesic (dose & ROA)**	**Testing specifications**	**Effect on pain measures**
Wolff et al. 1966[S15]	Crossover, placebo-controlled	Morphine (10 mg im)	Cold pressor test	No effect on pain threshold, increase in pain tolerance, decrease in pain sensitivity
Jarvik et al. 1981[S16]	Crossover, placebo-controlled	Morphine (10 mg/70 kg iv)	Cold pressor test	Increase of pain detection threshold and pain tolerance (tolerance > detection threshold)
Posner et al. 1985[S17]	Double-blind, placebo-controlled, crossover	Dipipanone (2mg, 4mg, 8mg po)	Cold pressor test	Decrease in pain ratings for 4mg and 8mg dipipanone
Holland et al. 1987[S18]	Double-blind, placebo-controlled, crossover	Dipipanone (8mg po)	Cold pressor test	Decrease in pain intensity ratings
Cleeland et al. 1996[S19]	Double-blind, active placebo controlled	Morphine (0.214 mg/kg po, 0.286 mg/kg po, 0.357 mg/kg po, 0.429 mg/kg po)	Cold pressor test	No effect on pain intensity and unpleasantness ratings, increase in pain tolerance for highest dose morphine
Gustorff et al. 2003[S3]	Double-blind, active placebo controlled	Remifentanil (0.08 µg/kg*min)	Contact cold on skin	No effect on pain detection thresholds and pain tolerance

Naef et al. 2003[S4]	Double-blind, (active) placebo-controlled	Morphine (30 mg po)	Cold pressor test	Decrease in pain intensity ratings, increase in pain tolerance
Eisenberg et al. 2010[S9]	Double-blind, active placebo controlled	Oxycodone (0.3mg/kg po)	Cold pressor test	Decrease in pain intensity ratings, increase in pain tolerance
Eisenberg et al. 2010[S9]	Double-blind, active placebo controlled	Oxycodone (0.3mg/kg po)	Contact cold on skin	No effect on pain detection threshold
Andresen et al. 2011[S10]	Double-blind, placebo-controlled, crossover	Fentanyl (25 µg/h, transdermal), Buprenorphine (20 µg/h, transdermal)	Cold pressor test	Decrease of pain intensity ratings
Angst et al. 2012[S11]	Double-blind, placebo-controlled	Alfentanil (100 ng/ml plasma concentration iv)	Cold pressor test	Increase of pain detection threshold and pain tolerance
Olesen et al. 2014[S13]	Double-blind, placebo-controlled, crossover	Morphine (30 mg po)	Cold pressor test	Decrease of pain intensity ratings
Winchester et al. 2014[S20]	Double-blind, crossover (dose scalation for PF-05105679)	Oxycodone (20 mg po)	Cold pressor test	Decrease of pain intensity ratings
Kleine-Borgmann et al. 2021[S21]	Double-blind, placebo-controlled	Tilidin/Naloxone (100/8, 150/4 mg po)	Cold pressor test	Decrease of pain intensity ratings, increase of pain tolerance
Watso et al. 2022[S22]	Blinded, placebo-controlled, crossover	Fentanyl (0.075 mg iv)	Cold pressor test	Decrease of pain intensity ratings

These studies explored mostly prolonged exposure to noxious cold. Opioids show analgesic efficacy in the majority of those studies, with more consistent effect on pain tolerance than pain thresholds. Studies that employ contact cold (superficial tissue) do not show an analgesic effect of opioids.

Table S3. Efficacy of systemic opioids on human experimental pressure pain, related to Figure 5, Introduction, and Discussion.

Author, year	**Study specifics**	**Analgesic (dose & ROA)**	**Testing specifications**	**Effect on pain measures**
Naef et al. 2003[S4]	Double-blind, (active) placebo-controlled	Morphine (30 mg po)	Finger pulp	Increase in pain tolerance
Fillingim et al. 2005[S7]	Double-blind, placebo-controlled, crossover	Morphine (0.08mg/kg iv)	Muscle and bone	Increase in pain thresholds

Arendt-Nielsen et al. 2009[S8]	Double-blind, (active) placebo-controlled, crossover	Oxycodone (15 mg po)	Muscle	No effect on pain thresholds and pain tolerance
Andresen et al. 2011[S10]	Double-blind, placebo-controlled, crossover	Fentanyl (25 µg/h, transdermal), Buprenorphine (20 µg/h, transdermal)	Bone	No effect on pain tolerance (Fentanyl), increase in pain tolerance (Buprenorphine)
King et al. 2013[S12]	Double-blind, (active) placebo-controlled, crossover	Morphine (0.08mg/kg iv), Pentazocine (0.5 mg/kg iv)	Muscle, bone	Increase in pain threshold
Olesen et al. 2014[S13]	Double-blind, placebo-controlled, crossover	Morphine (30 mg po)	Muscle, bone, rectal	Increase of pain tolerance (all testing locations)
Prosenz & Gustorff 2017[S14]	Double-blind, (active) placebo-controlled, crossover	Fentanyl (1 µg/kg iv)	Muscle	Increase in pain threshold

These studies used sustained, increasing pressure stimulation to skin and underlying deep tissues. Opioids show analgesic efficacy in the majority of those studies.

Table S4. Efficacy of systemic opioids on human experimental ischemic pain, related to Figure 5, Introduction, and Discussion.

Author, year	**Study specifics**	**Analgesic (dose & ROA)**	**Testing specifications**	**Effect on pain measures**
Fillingim et al. 2005[S7]	Double-blind, placebo-controlled, crossover	Morphine (0.08mg/kg iv)	Modified submaximal tourniquet procedure	Increase in pain thresholds and pain tolerance, decrease in pain and unpleasantness ratings
Arendt-Nielsen et al. 2009[S8]	Double-blind, (active) placebo-controlled, crossover	Oxycodone (15 mg po)	Tourniquet procedure	Increase in pain thresholds and pain tolerance
King et al. 2013[S12]	Double-blind, (active) placebo-controlled, crossover	Morphine (0.08mg/kg iv), Pentazocine (0.5 mg/kg iv)	Modified submaximal tourniquet procedure	Increase in pain thresholds and pain tolerance

These studies used a sustained tourniquet to induce ischemic pain. Opioids showed efficacy on both pain thresholds and pain tolerance.

Table S5. Efficacy of systemic opioids on other human experimental pain models, related to Figure 6, Introduction, and Discussion.

Author, year	Study specifics	Analgesic (dose & ROA)	Testing specifications	Effect on pain measures
Andresen et al. 2011[S10]	Double-blind, placebo-controlled, crossover	Fentanyl (25 µg/h, transdermal), Buprenorphine (20 µg/h, transdermal)	Intramuscular NGF injection, pressure testing post-injection	No effect on pressure tolerance thresholds (Fentanyl), increase in pressure tolerance thresholds (Buprenorphine)
Arendt-Nielsen et al. 2009[S8]	Double-blind, (active) placebo-controlled, crossover	Oxycodone (15 mg po)	Skin pinch, esophageal pressure	Pinch: Increase in pain tolerance Esophageal pressure: Increase in pain detection threshold and moderate pain threshold

NGF-induced muscle soreness (sustained stimulus, deep tissue) was partially responsive to opioids. An opioid agonist showed efficacy with prolonged noxious mechanical stimulation of superficial and visceral tissue.

Table S6. Intrathecal opioids and clinical pain, related to Figure 7, Introduction, and Discussion.

Author, year	Study specifics	Clinical Indication	Analgesic	Effect on pain
Samii et al. 1979[S23]	No placebo control	Intractable cancer pain (mixed pain)	Morphine (1-3 mg it), Pethidine (10-30 mg it)	Complete analgesia
Wang et al. 1979[S24]	Double-blind, placebo control	Intractable cancer pain (mixed pain)	Morphine (0.5 mg, 1.0 mg it)	Complete analgesia
Baraka et al. 1981[S25]	No placebo control	First stage labor pain	Morphine (1mg, 2mg it)	Complete analgesia
Gray et al. 1986[S26]	No placebo control	Postsurgical pain (thoracotomy)	Morphine (10 µg/kg it)	Excellent analgesia
Abboud et al. 1988[S27]	Double-blind, placebo control	Postsurgical pain (Cesarean section)	Morphine (0.25 mg, 0.1 mg it)	Analgesia, significantly stronger than placebo
Kirson et al. 1989[S28]	Double-blind, active control	Postsurgical pain	Morphine (0.1 mg, 0.2 mg it) Control: Lidocaine 75 mg it	Analgesia, significantly stronger than control for both dose levels
Leighton et al. 1989[S29]	No placebo control	Labor pain	Fentanyl (25 µg it) with Morphine (0.25 mg it)	Significant decrease in pain ratings
Cohen et al. 1993[S30]	No placebo control	First stage labor pain	Sufentanil (10 µg in 1ml it)	Analgesia

D'Angelo et al. 1994[S31]	Double-blind, active control	Labor pain	Sufentanil (10 µg in 2ml it) Control: Bupivacaine (30 mg epidural)	Significant decrease in pain ratings to control, high degree of patient satisfaction
Angel et al. 1998[S32]	No placebo control	"Failed back" pain (nociceptive and neuropathic pain), spinal cord damage	Morphine per intrathecal drug delivery system	Mixed results, 27% unresponsive
Schuchard et al. 1998[S33]	No placebo control	Nonmalignant chronic pain, nociceptive, neuropathic or mixed	Morphine per intrathecal drug delivery system	Pain reduction in all patients with nociceptive pain, partly in other pain etiologies (mixed > neuropathic)
Anderson et al. 1999[S34]	No placebo control	Nonmalignant chronic pain, nociceptive (3%), neuropathic (47%) or mixed (50%)	Morphine per intrathecal drug delivery system	Significant pain relief in 50% of patients
Gwirtz et al. 1999[S35]	No placebo control	Postsurgical pain	Morphine (0.2-0.8mg it)	High patient satisfaction with analgesia
Shaladi et al. 2007[S36]	No placebo control	Pain from vertebral fractures due to osteoporosis	Morphine per intrathecal drug delivery system	Clinically significant pain relief
Zacest et al. 2009[S37]	No placebo control	Refractory postherpetic neuralgia	Morphine per intrathecal drug delivery system	Partial pain relief
Fabiano et al. 2012[S38]	No placebo control	Postherpetic neuralgia	Morphine, Morphine + Bupivacaine, Sufentanil, Sufentanil + Bupivacaine, Sufentanil + Bupivacaine + Clonidine (intrathecal drug delivery systems)	Clinically significant pain reduction

Intrathecally applied opioids are very efficacious in relieving clinical nociceptive pain. Studies that included patients with neuropathic pain or a neuropathic pain component show mixed results. These studies provide functional support for our molecular-anatomically based findings of two main nociceptive populations: a population associated with sustained pain due to tissue damage (nociceptive pain) that expresses transcripts for the µ-opioid receptor, and a population that serves as a superficially located biowarning system and does not express transcripts for the µ-opioid receptor, hence, whose activity cannot be attenuated by clinically used opioids. These nociceptors contribute to neuropathic pain in rodents.[S39,S40] We therefore hypothesize that the poor responsiveness of neuropathic pain to opioids can be at least partially explained by the lack of µ-opioid receptor expression of these nociceptive fibers.

Table S7. Neuron population counts for experiment 1 (*TRPV1*, *OPRM1*, *OPRD1*, *OPRK1*), related to Figure 1.

	Donor 1	Donor 2	Donor 3	Donor 4
TRPV1+OPRM1+	99	77	95	124
TRPV1+OPRM1+OPRD1	68	77	64	68
TRPV1+OPRM1+OPRK1+	1	0	0	0
TRPV1+OPRM1+OPRD1+OPRK1+	0	4	2	3
TRPV1+	17	6	9	10
TRPV1+OPRD1+	91	83	79	50
TRPV1+OPRD1+OPRK1+	0	1	4	5
OPRM1+	5	9	0	6
OPRD1+	7	14	11	5
OPRM1+OPRD1+	3	7	3	5
no marker	48	40	39	41

This table presents the number of DRG neurons expressing individual marker combinations for each individual tissue donor. The most prevalent populations were further characterized. These results are shown in Figure 1.

Table S8. Neuron population counts for experiment 2 (*TRPV1*, *OPRM1*, *OPRL1*, *SPP1*), related to Figure 2.

	Donor 1	Donor 2	Donor 3	Donor 4
TRPV1+OPRM1+	98	93	50	80
TRPV1+OPRM1+OPRL1+	90	72	117	117
TRPV1+OPRM1+OPRL1+SPP1+	9	9	5	2
TRPV1+	79	68	83	74
TRPV1+OPRL1+	7	12	13	11
TRPV1+OPRL1+SPP1+	5	6	13	4
OPRM1+OPRL1+	4	0	0	1
OPRM1+OPRL1+SPP1+	2	1	1	0
SPP1+	4	13	1	0
OPRL1+SPP1+	28	33	26	37
no marker	1	2	2	4

This table presents the number of DRG neurons expressing individual marker combinations for each individual tissue donor. The most prevalent populations were further characterized. These results are shown in Figure 2.

Table S9. Neuron population counts for experiment 3 (*TRPV1, OPRM1, SCN10A, SCN11A*), related to Figure 3.

	Donor 1	Donor 2	Donor 3	Donor 4
TRPV1+OPRM1+	3	1	1	2
TRPV1+OPRM1+SCN10A+	1	1	5	4
TRPV1+OPRM1+SCN11A+	6	6	7	6
TRPV1+OPRM1+SCN10A+SCN11A+	164	177	164	197
TRPV1	5	7	7	2
TRPV1+SCN10A+	0	1	1	0
TRPV1+SCN11A+	0	5	2	2
TRPV1+SCN10A+SCN11A+	97	90	91	94
OPRM1+SCN11A+	2	0	3	2
OPRM1+SCN10A+SCN11A+	0	1	0	3
OPRM1+	0	0	1	1
SCN11A+	0	1	0	0
no marker	55	34	29	29

This table presents the number of DRG neurons expressing individual marker combinations for each individual tissue donor. The most prevalent populations were further characterized. These results are shown in Figure 3.

Table S10. Neuron population counts for experiment 4 (*TRPV1, OPRM1, TRPA1, TAC1*), related to Figure 4.

	Donor 1	Donor 2	Donor 3	Donor 4
TRPV1+OPRM1+	86	47	67	98
TRPV1+OPRM1+TAC1+	22	68	42	45
TRPV1+OPRM1+TRPA1+TAC1+	63	64	57	32
TRPV1+OPRM1+TRPA1+	30	17	8	30
TRPV1+	37	28	30	25
TRPV1+TRPA1+	54	52	41	39
TRPV1+TAC1+	2	5	2	3
TRPV1+TRPA1+TAC1+	0	0	2	0
OPRM1+	6	10	9	8
TAC1+	1	2	0	0
no marker	39	56	57	32

This table presents the number of DRG neurons expressing individual marker combinations for each individual tissue donor. The most prevalent populations were further characterized. These results are shown in Figure 4.

Table S11. Neuron population counts for experiment 5 (*TRPV1*, *OPRM1*, *TRPA1*, *TRPM8*), related to Figure S6.

	Donor 1	Donor 2	Donor 3	Donor 4
TRPV1+OPRM1+	46	48	28	37
TRPV1+OPRM1+TRPA1+	20	28	11	19
TRPV1+OPRM1+TRPM8+	40	43	52	70
TRPV1+OPRM1+TRPA1+TRPM8+	54	56	60	96
TRPV1+	41	27	42	17
TRPV1+TRPA1+	64	50	53	52
TRPV1+TRPM8+	0	3	7	5
TRPV1+TRPA1+TRPM8+	5	2	1	1
OPRM1+	5	11	7	12
OPRM1+TRPA1+	0	1	0	1
OPRM1+TRPM8+	0	6	12	1
OPRM1+TRPA1+TRPM8+	0	2	0	0
TRPA1+	2	1	0	0
TRPM8+	0	3	3	1
TRPA1+TRPM8+	0	0	0	1
no marker	34	42	51	36

This table presents the number of DRG neurons expressing individual marker combinations for each individual tissue donor. The most prevalent populations were further characterized. These results are shown in Figure S6.

Table S12. Neuron population counts for experiment 6 (*TRPV1*, *OPRM1*, *PIEZO2*, *P2RX3*), related to Figure 5.

	Donor 1	Donor 2	Donor 3	Donor 4
TRPV1+OPRM1+	10	25	9	15
TRPV1+OPRM1+P2RX3+	68	51	54	56
TRPV1+OPRM1+PIEZO2+	1	1	0	4
TRPV1+OPRM1+PIEZO2+P2RX3+	71	92	116	122
TRPV1+	0	3	0	1
TRPV1+PIEZO2+	2	2	6	4
TRPV1+P2RX3+	4	3	2	0
TRPV1+PIEZO2+P2RX3+	84	71	77	62
OPRM1+PIEZO2+	6	1	2	0
OPRM1+PIEZO2+P2RX3+	13	7	1	3
PIEZO2+P2RX3+	2	3	11	4
PIEZO2+	55	46	39	45
no marker	0	5	5	0

This table presents the number of DRG neurons expressing individual marker combinations for each individual tissue donor. The most prevalent populations were further characterized. These results are shown in Figure 5.

Table S13. Neuron population counts for experiment 7 (*TRPV1, OPRM1, NTRK1, GFRA2*), related to Figure 6.

	Donor 1	Donor 2	Donor 3	Donor 4
TRPV1+OPRM1+	28	26	42	34
TRPV1+OPRM1+NTRK1+	153	104	136	141
TRPV1+OPRM1+NTRK1+GFRA2+	19	17	7	8
TRPV1+OPRM1+GFRA2	4	2	6	5
TRPV1+	10	8	8	2
TRPV1+NTRK1+	3	17	8	5
TRPV1+GFRA2+	67	59	67	82
TRPV1+NTRK1+GFRA2+	1	2	3	0
OPRM1+	8	1	2	6
OPRM1+NTRK1+	4	3	9	6
OPRM1+GFRA2+	0	2	0	0
OPRM1+NTRK1+GFRA2+	1	0	1	1
NTRK1+	1	1	5	0
NTRK1+GFRA2+	1	0	0	0
GFRA2+	5	23	12	4
no marker	32	44	16	36

This table presents the number of DRG neurons expressing individual marker combinations for each individual tissue donor. The most prevalent populations were further characterized. These results are shown in Figure 6.

Table S14. Neuron population counts for experiment 8 (*TRPV1, OPRM1, GFRA2, MRGPRD*), related to Figure 6.

	Donor 1	Donor 2	Donor 3	Donor 4
TRPV1+OPRM1+	156	171	188	159
TRPV1+OPRM1+GFRA2+	8	3	20	16
TRPV1+OPRM1+MRGPRD+	0	3	0	8
TRPV1+OPRM1+GFRA2+MRGPRD+	0	1	0	3
TRPV1+	6	12	9	9
TRPV1+GFRA2+	13	31	14	13
TRPV1+MRGPRD+	3	0	0	0
TRPV1+GFRA2+MRGPRD+	89	30	60	54
OPRM1+	3	8	1	10
OPRM1+GFRA2+	7	0	1	5
GFRA2+	6	1	7	27
no marker	34	55	9	18

This table presents the number of DRG neurons expressing individual marker combinations for each individual tissue donor. The most prevalent populations were further characterized. These results are shown in Figure 6.

Table S15. Clinical trials involving agonists to non-μ-opioid receptors, related to Figure 1 and Discussion.

Drug name	Action	Clinical trial #	Phase	Clinical indication	Status
ADL5859	selective nonpeptide δ-opioid receptor agonist	NCT00993863	Phase 2	Acute pain after third molar extraction	completed 2007
ADL5859	selective nonpeptide δ-opioid receptor agonist	NCT00626275	Phase 2	Pain from rheumatoid arthritis	completed 2008
ADL5859	selective nonpeptide δ-opioid receptor agonist	NCT00603265	Phase 2	Pain from diabetic peripheral neuropathy	completed 2008
ADL5859	selective nonpeptide δ-opioid receptor agonist	NCT00979953	Phase 2	Pain from knee osteoarthritis	completed 2010
ADL5747	selective nonpeptide delta agonist	NCT00979953	Phase 2	Pain from knee osteoarthritis	completed 2010
ADL5747	selective nonpeptide δ-opioid receptor agonist	NCT01058642	Phase 2	Pain from postherpetic neuralgia	terminated 2010
NP2	gene-transfer vector for proenkephalin	NCT01291901	Phase 2	Intractable cancer pain	completed 2013
Asimadoline (EMD 61753)	second-generation peripheral κ-opioid receptor agonist	NCT00454688	Phase 2	Pain from inflammatory bowel syndrome	completed 2007
Asimadoline (EMD 61753)	second-generation peripheral κ-opioid receptor agonist	NCT00955994	Phase 2	Pain from inflammatory bowel syndrome	completed 2007
Asimadoline (EMD 61753)	second-generation peripheral κ-opioid receptor agonist	NCT00443040	Phase 2	Ileus after colon resections	completed 2008
Asimadoline (EMD 61753)	second-generation peripheral κ-opioid receptor agonist	NCT01100684	Phase 3	Pain from diarrhea dominant inflammatory bowel syndrome	completed 2013
Asimadoline (EMD 61753)	second-generation peripheral κ-opioid receptor agonist	NCT02475447	Phase 2	Pruritus from atopic dermatitis	completed 2017
Difelikefalin (CR845)	third-generation peripheral κ-opioid receptor agonist	NCT00877799	Phase 2	Post-hysterectomy pain	completed 2010
Difelikefalin (CR845)	third-generation peripheral κ-opioid receptor agonist	NCT01361568	Phase 2	Post-hysterectomy pain	completed 2012
Difelikefalin (CR845)	third-generation peripheral κ-opioid receptor agonist	NCT01789476	Phase 2	Post-bunionectomy pain	completed 2013
Difelikefalin (CR845)	third-generation peripheral κ-opioid receptor agonist	NCT02524197	Phase 2	Pain from knee or hip osteoarthritis	completed 2016
Difelikefalin (CR845)	third-generation peripheral κ-opioid receptor agonist	NCT02944448	Phase 2	Pain from knee or hip osteoarthritis	completed 2017

Difelikefalin (CR845)	third-generation peripheral κ-opioid receptor agonist	NCT02542384	Phase 2/Phase 3	Post-abdominal surgery pain	completed 2018
Difelikefalin (CR845)	third-generation peripheral κ-opioid receptor agonist	NCT03636269	Phase 3	Pruritus in hemodialysis patients	completed 2020, approved by FDA 2021
Difelikefalin (CR845)	third-generation peripheral κ-opioid receptor agonist	NCT03422653	Phase 3	Pruritus in hemodialysis patients	completed 2020, approved by FDA 2021
Difelikefalin (CR845)	third-generation peripheral κ-opioid receptor agonist	NCT04018027	Phase 2	Pruritus in atopic dermatitis	completed 2021
Difelikefalin (CR845)	third-generation peripheral κ-opioid receptor agonist	NCT04706975	Phase 2	Pruritus in notalgia paresthetica	completed 2022
Difelikefalin (CR845)	third-generation peripheral κ-opioid receptor agonist	NCT03995212	Phase 2	Pruritus in primary biliary cholangitis	terminated 2022
Difelikefalin (CR845)	third-generation peripheral κ-opioid receptor agonist	NCT05356403	Phase 3	Pruritus in chronic kidney disease without dialysis	terminated 2024
Difelikefalin (CR845)	third-generation peripheral κ-opioid receptor agonist	NCT05387707	Phase 3	Adjunct to topical corticoids for pruritus in atopic dermatitis	terminated 2024
Cebranopadol	full agonist on μ- and δ-opioid receptor, partial agonist on nociceptin-receptor and κ-opioid receptor	NCT01964378	Phase 3	Chronic moderate to severe pain related to cancer	completed 2015
Cebranopadol	full agonist on μ- and δ-opioid receptor, partial agonist on nociceptin-receptor and κ-opioid receptor	NCT01939366	Phase 3	diabetic neuropathy	completed 2015

Multiple entries of certain agents tested in clinical trials presumably reflect a developmental evolution of compounds that initially began as analgesics**.**

Table S16. Human donor information, related to Methods.

Donor No.	Gender	Age	Cause of death	Medical conditions	Retrieval time (h:min)
1	M	27	CVA / ICH / Stroke	N/A	3:16
2	F	21	Anoxia / Drug Intoxication	Seizures, Bipolar, difficulty walking	2:02
3	F	22	Anoxia / Drug Intoxication	N/A	8:12
4	M	20	CVA / ICH / Stroke	N/A	3:10

Table S17. Advanced Cell Diagnostics (ACD) RNAscope probes, related to Methods.

mRNA	Gene name	ACD Cat No.
GFRA2	GDNF Family Receptor Alpha 2	463011
MRGPRD	MAS Related GPR Family Member D	524871
NTRK1	Neurotrophic Receptor Tyrosine Kinase 1	402631
OPRD1	opioid receptor delta 1	536061
OPRK1	opioid receptor kappa 1	1148211
OPRK1	opioid receptor kappa 1	1148211-O1 (custom 13 ZZ probe)
OPRL1	opioid related nociceptin receptor 1	536071
OPRM1	opioid receptor mu 1	410681
PIEZO2	piezo type mechanosensitive ion channel component 2	449951
P2RX3	purinergic receptor P2X 3	406301
SCN10A	sodium voltage-gated channel alpha subunit 10	406291
SCN11A	sodium voltage-gated channel alpha subunit 11	404791
SPP1	secreted phosphoprotein 1	420101
TAC1	tachykinin precursor 1	310711
TRPA1	transient receptor potential cation channel subfamily A member 1	503741
TRPM8	transient receptor potential cation channel subfamily M member 8	543121
TRPV1	Transient receptor potential cation channel subfamily V member 1	415381

Table S18. Fluorophores for TSA-RNAscope V2 imaging, related to Methods.

Fluorophore	Exciter	Dichroic	Emitter
DAPI	FF01-340/26	FF458-Di02	FF01-482/25
Opal 520	FF01-494/20	FF506-Di03	FF01-527/20
Opal 570	FF01-535/22	FF560-Di01	FF01-580/23
Opal 620	FF01-586/20	FF605-Di02	FF01-628/32
Opal 690	FF01-680/22	FF705-Di01	FF01-720/13

Figure S1. Puncta counts and signal intensities correlate, despite variability in puncta brightness, related to Methods.

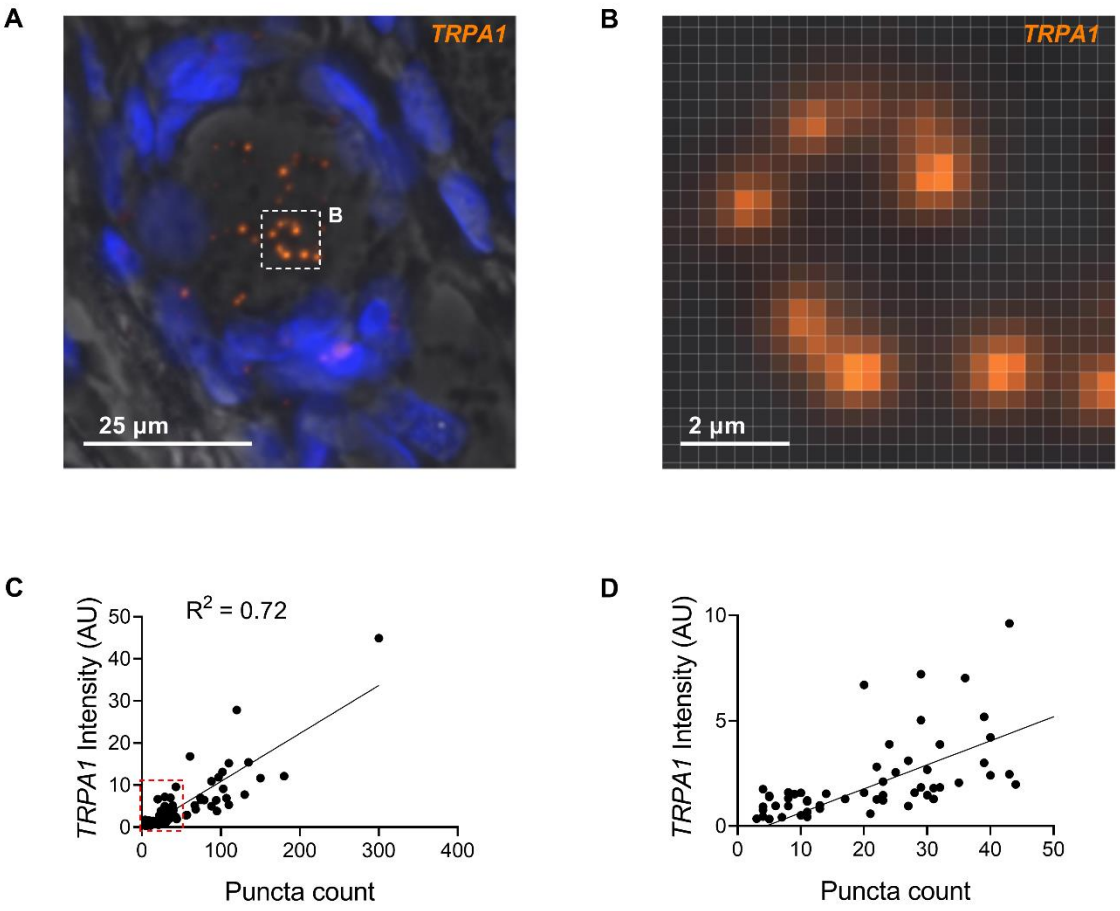

(A) Representational neuron expressing *TRPA1* (see also Figure S6). Each puncta represents a mRNA. Signal was enhanced for visibility. Tissue was visualized with differential interference contrast (DIC) imaging. (B) Pixel-level resolution of *TRPA1* puncta shown in white square in (A). Note the dimensions of puncta (at least 2x2 pixel, or 0.67x0.67 µm). Due to the TSA amplification puncta can vary in brightness and size. (C) Correlation between puncta count and signal intensity (mean grey scale as calculated by Fiji). 80 neurons were included in the analysis (n=20 neurons from each donor). Puncta count and signal intensity show a strong correlation, despite the variation in puncta brightness and size. (D) Data shown in (C), restricted to puncta counts n≤50.

Figure S2. Regions of Interest (ROIs) to measure neuronal cell size, transcript signal intensity, and signal bleed, related to Methods.

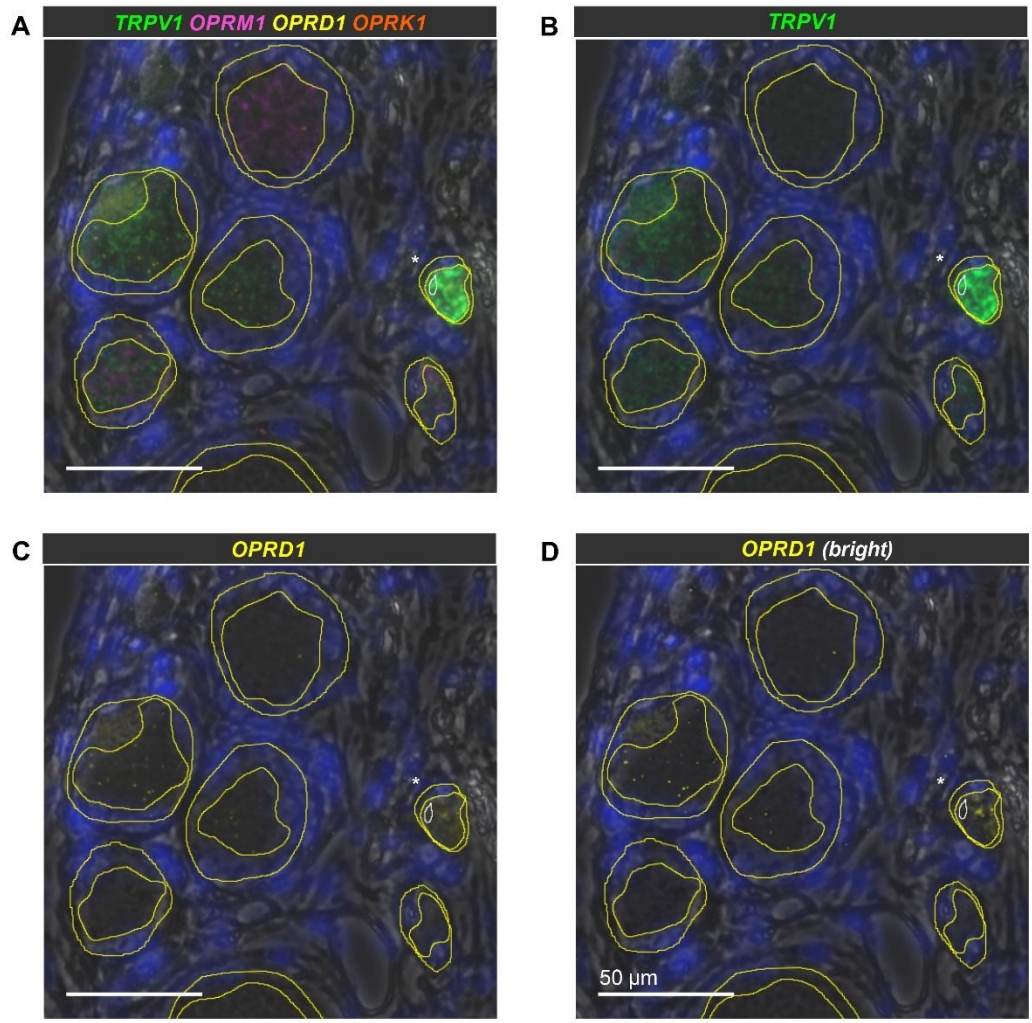

(A) Representative section of human DRG showing positive transcripts for *TRPV1*, *OPRM1*, *OPRD1*, and *OPRK1* in a multichannel overlay (experiment 1, unmanipulated signal). (B) Window showing transcripts for *TRPV1* (unmanipulated signal). Window showing transcripts for *OPRD1* with unmanipulated signal (C) and signal that was adjusted for brightness and contrast for visibility (D). Outer yellow circles represent ROIs to determine neuronal cells size and inner yellow circles ROIs to calculate transcript expression intensity (following the cytoplasm outline and excluding lipofuscin). In case signal bleed was visually detected (here from *TRPV1* (green, 488 nm channel) to *OPRD1* (yellow, 456 nm channel) in the neuron marked with an asterisk), we used the bleed signal intensity of a separate ROI capturing bleed signal (white circle) for correction. Tissue was visualized with differential interference contrast (DIC) imaging.

Figure S3. Percentage of *TRPV1+OPRM1+* nociceptors across experiments and percentage of *TRPV1+OPRM1+* nociceptors across experiments stratified by gender, related to Figure 1.

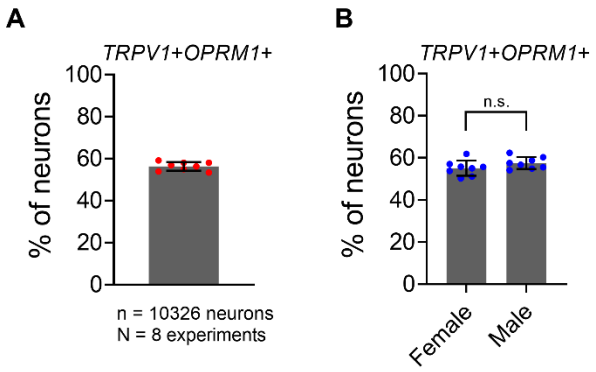

(A) Percentage of neurons showing transcripts for both *TRPV1* and *OPRM1* across all in situ hybridization experiments (N=8 experiments). Bar graph represents mean percentage of *TRPV1+OPRM1+* neurons of all experiments and all donors, error bars represent standard deviation, and dots show mean percentage of *TRPV1+OPRM1+* neurons for all donors per individual experiment ($\bar{x}$=56.3±2.1%). (B) Percentage of *TRPV1+OPRM1+* neurons across all in situ hybridization experiments (N=8 experiments) stratified by gender ($\bar{x}$=55.1±3.6% for Females, $\bar{x}$=57.5±2.8% for Males). We did not detect a gender difference for the prevalence of *TRPV1+OPRM1+* nociceptors (p=0.2, Mann-Whitney U test). The small sample of tissue donors and the fact that both female donors died of a drug overdose, as opposed to the two male tissue donors, limits the interpretation of this result. Bar graphs represent mean percentage of *TRPV1+OPRM1+* neurons of all experiments and gender-stratified donors (2 Females, 2 Males), error bars represent standard deviations, and dots show mean percentage of *TRPV1+OPRM1+* neurons per individual experiment for donors stratified by gender.

Figure S4. Neuronal subpopulations expressing *OPRK1*, related to Figure 1.

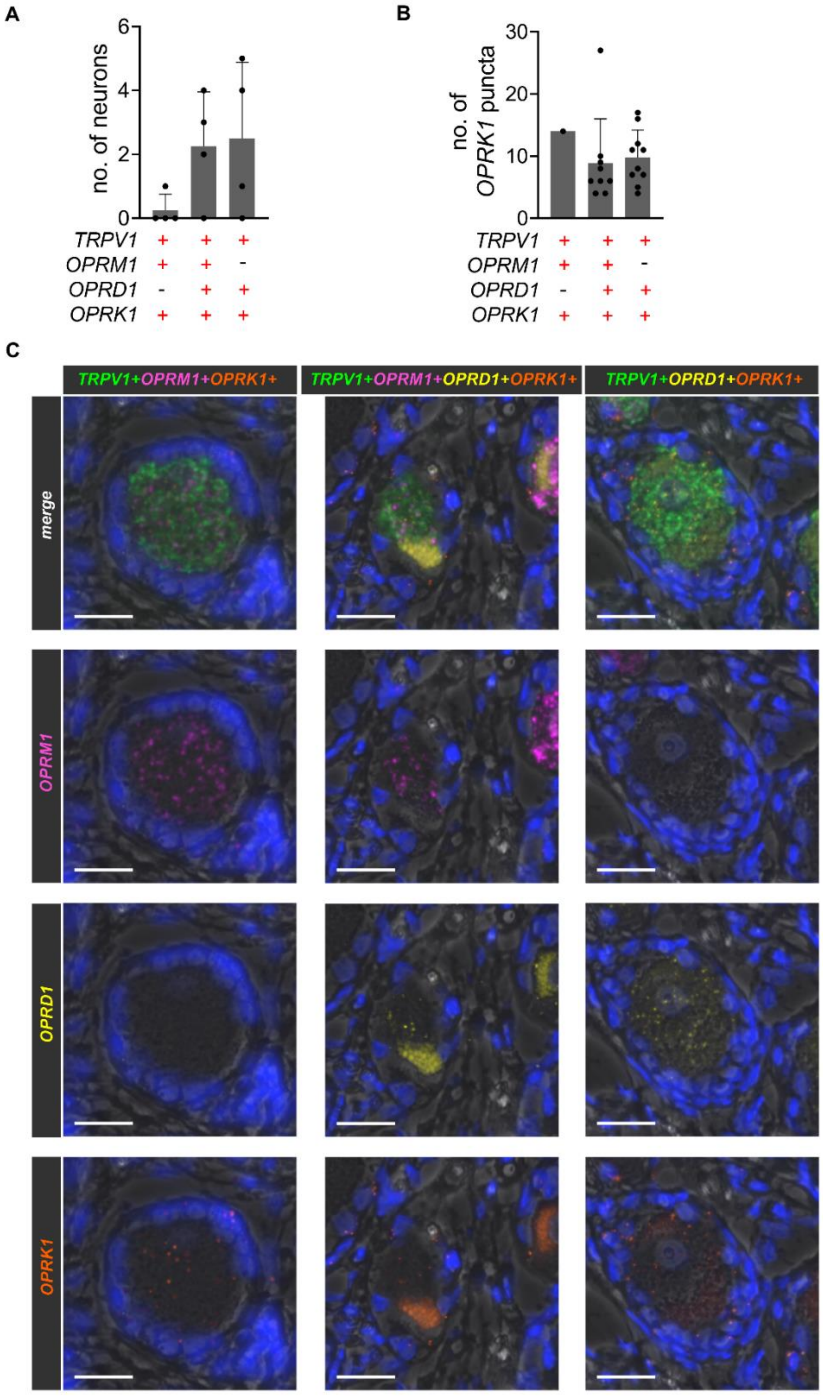

(A) We detected transcripts for *OPRK1* in 20/1280 neurons. All *OPRK1*-expressing neurons co-expressed *TRPV1* and transcripts for at least one other opioid receptor. Bar graphs demonstrate mean counts, standard deviation and individual counts for each donor. (B) *OPRK1* puncta counts for each *OPRK1*-expressing subpopulation. *OPRK1* was expressed in a low fashion in those neurons, with 13/20 neurons expressing 10 transcripts or less. (C) Representative neuron of each subpopulation shown in an overlay and individual channels for each opioid-receptor transcript. Signal was adjusted for brightness and contrast for visibility. Tissue was visualized with differential interference contrast (DIC) imaging. Scale bars represent 25 µm.

Figure S5. Spatial overlap of transcripts for *OPRK1* as detected with the custom and standard probe, respectively, related to Figure 1.

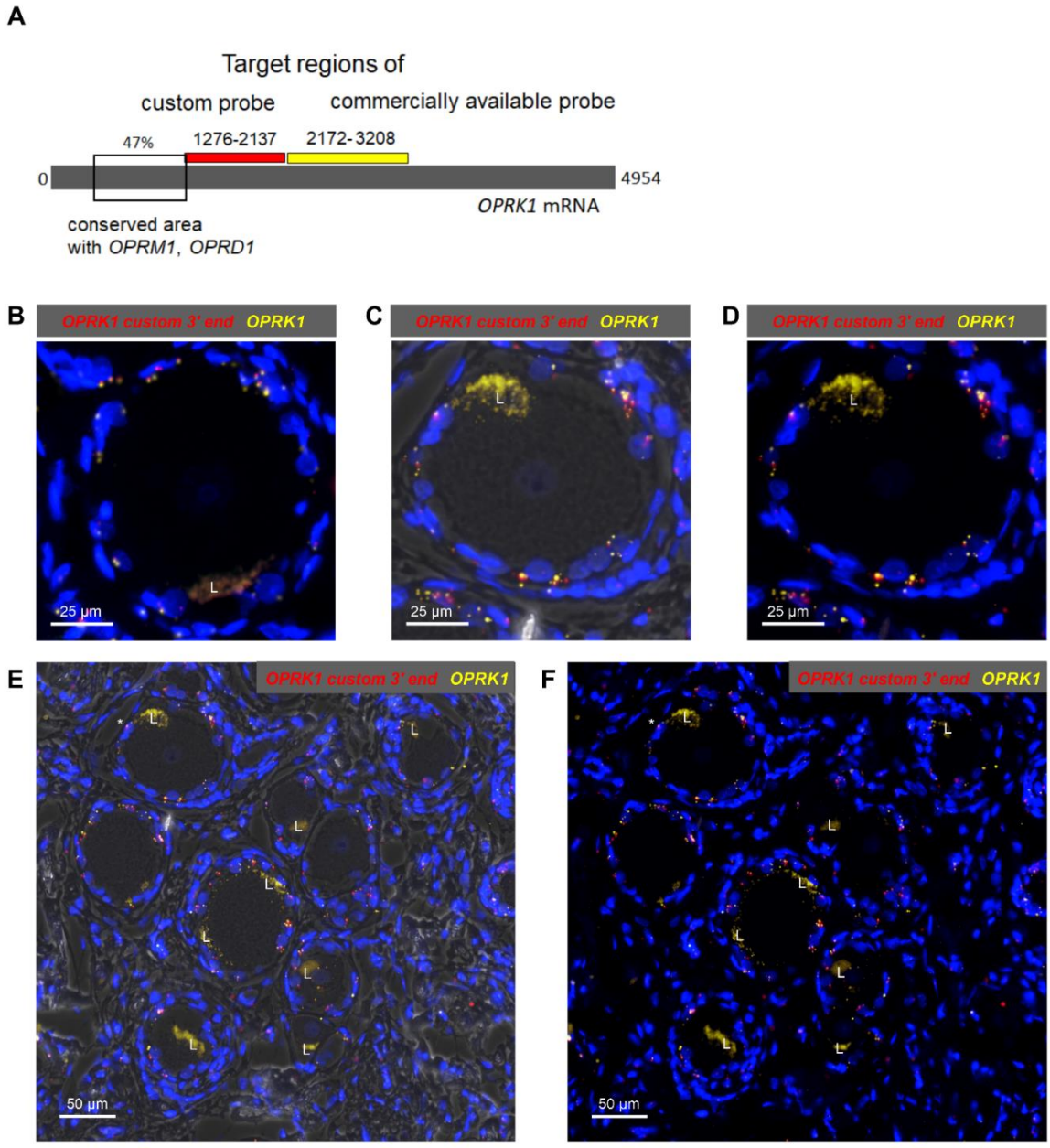

(A) Schematic illustration of the *OPRK1* transcript and target areas for the custom probe (red) and the commercially available probe (yellow). Note that the target areas for both probes do not overlap. The custom probes are not predicted to cross react with other isoforms based on sequence differences between the target regions. Note that this is also confirmed empirically in co-labeling studies. (B) Same single neuron as shown in Figure 1F). (C) and (D) Example of a single neuron (marked by an asterisk in (E) and (F)). (E) and (F) Representative windows showing a larger field. (C) and (E) include tissue visualized with differential interference contrast (DIC) imaging. Transcripts for *OPRK1* as detected with the custom probe are illustrated in red, and with the standard probe in yellow. Lipofuscin is marked with an "L".

Figure S6. *OPRM1*-positive nociceptors express *TRPM8*, related to Figure 7 and Results.

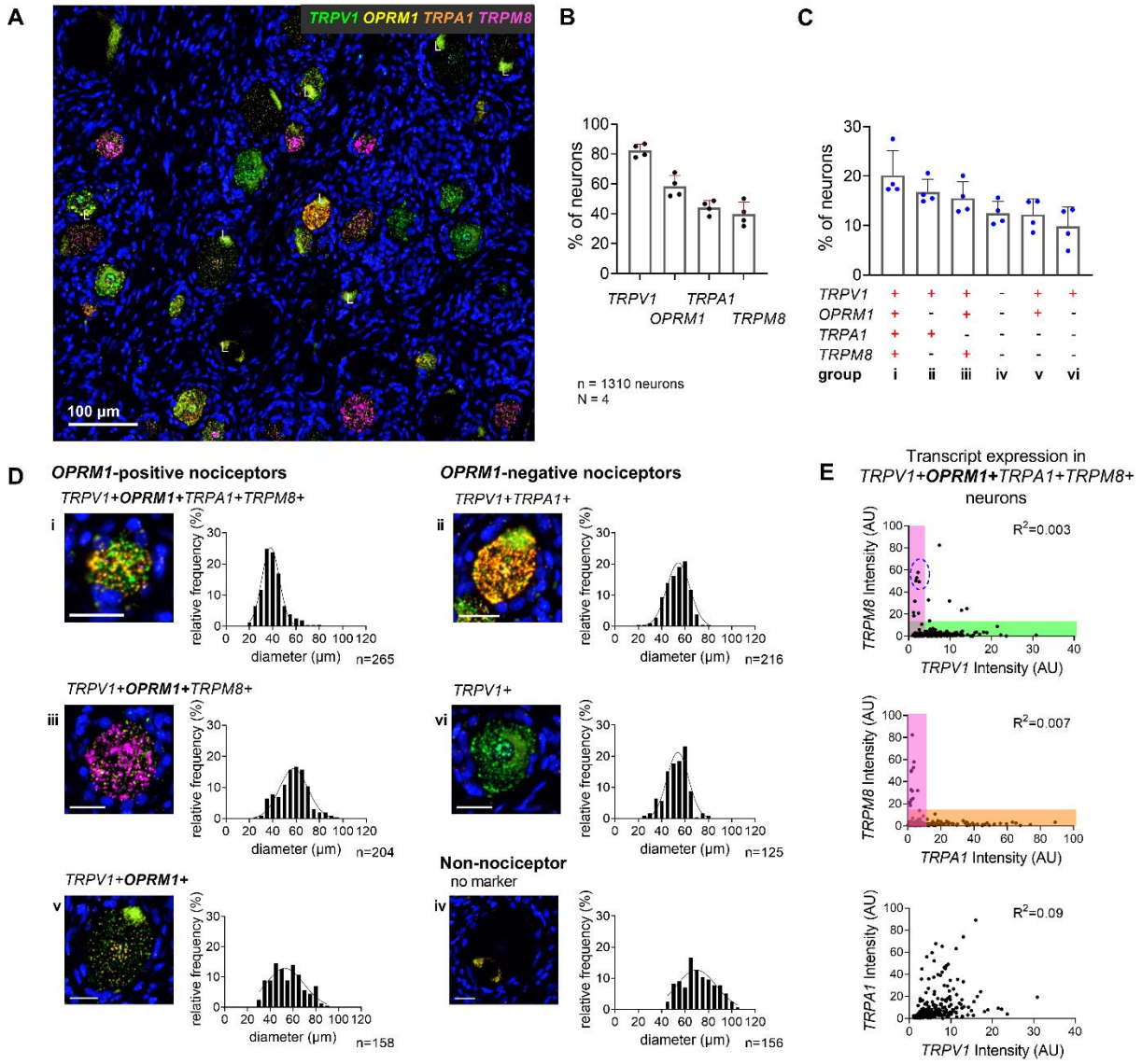

(A) Representative section of human DRG showing neurons expressing transcripts for TRPV1, the µ-opioid receptor (*OPRM1*), the chemo-sensitive receptor TRPA1 and the cold-sensitive receptor TRPM8. (B) Percentage of 1,310 neurons expressing each individual transcript. (C) Percentage of neurons expressing the most common transcript combinations. Bar graphs in (B) and (C) show mean, SD, and individual values from all four donors. (D) Multi-channel microscopy images of a representative individual neuron of each population and the population's cell size distribution. Scale bars = 25 µm. Lipofuscin is marked with an "L". (E) Correlation analyses for expression intensities of the transient receptor channels in the quad+ population i. While there is co-expression for all transcripts within this population, the high-*TRPM8* expressing subpopulation expresses low *TRPV1* and *TRPA1*, indicating a distinct population of strongly cold-responsive neurons (blue oval). The small-diameter *TRPV1+OPRM1+TRPA1+TAC1+* quad+ population identified in experiment 4 (Figure 4Eii) is a multimodal, highly noci-responsive population that overlaps with the quad+ population in this experiment. The detection of *TRPM8* expression contributes the sensation of cold in this population.

Figure S7. Classification of *TRPV1+OPRM1+* nociceptors and *TRPV1+OPRM1-* nociceptors into C- and A-nociceptors, related to Figure 7.

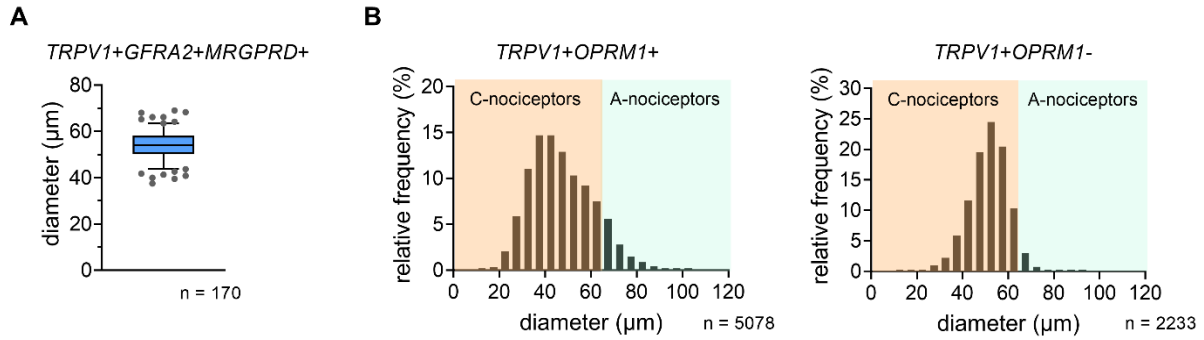

(A) Box plot of neuronal diameter for the molecularly defined *TRPV1+GFRA2+MRGPRD+* C-nociceptive population (see Figure 7I). [S41,42] Whiskers represent 5th (x=43.8 µm) and 95th (x=63.3 µm) percentile, respectively. Single dots represent data points beyond the 5th and 95th percentile. (B) Histograms of *TRPV1+OPRM1+* and *TRPV1+OPRM1-* nociceptors. Based on the cell size distribution of *TRPV1+GFRA2+MRGPRD+* neurons in (A,) which are a subpopulation of *TRPV1+OPRM1-* neurons, we estimated that neurons with a cell diameter ≤65 µm likely represent C-nociceptors, and those with a cell diameter >65 µm likely represent A-nociceptors.

Figure S8. Comparison of human DRG in situ hybridization results from this study with spatial transcriptomic data; related to Figure 1 and Discussion.

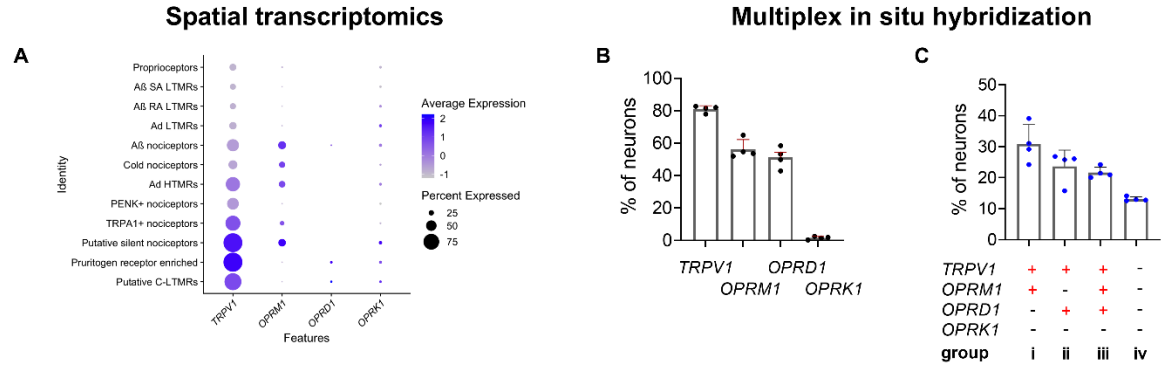

(A) Dot plots demonstrating gene expression in different clusters as provided by spatial transcriptomics study.[S43] (B) Percentage of neurons expressing each individual gene and (C) percentage of neurons expressing the most common transcript combinations. In (A), note that the expression of *OPRM1* is not unambiguously described, that a co-expression with *OPRD1* in some populations of nociceptors is not detected, and that *OPRK1* is expressed in all populations. These findings are overly inclusive compared to the discrete co-expression patterns obtained with our methodology. We show co-expression of *OPRM1* with *OPRD1* in a subgroup of *TRPV1+OPRM1+* nociceptors and that *OPRK1* was hardly expressed by DRG neurons, but broadly by satellite glial cells (Figures 1F, S4, S5). It is notable, that both *OPRD1* and *OPRK1* exhibit low transcript levels, which may be one reason why they are prone to drop-out in sc/sn sequencing and/or misclassification in spatial transcriptomics.

Figure S9. Comparison of human DRG in situ hybridization results from this study with spatial transcriptomic data; related to Figure 2 and Discussion.

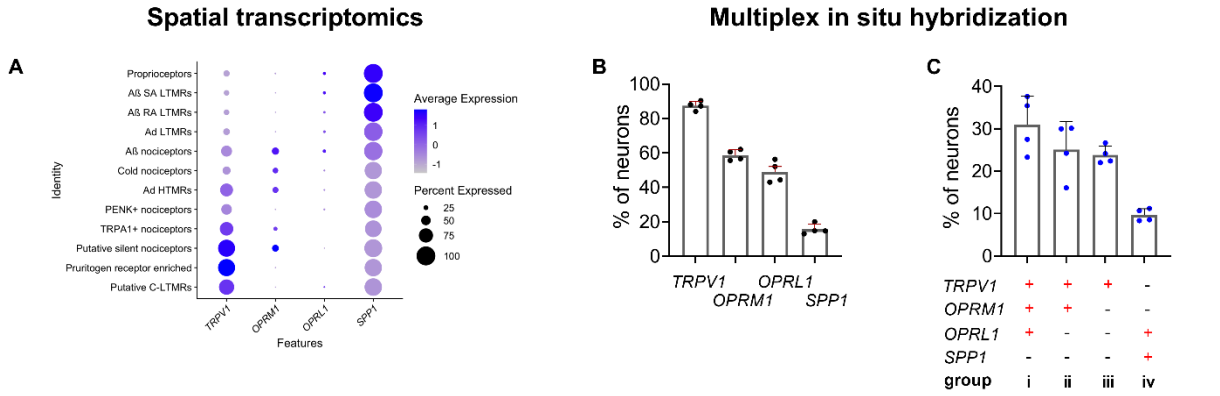

(A) Dot plots demonstrating gene expression in different clusters as provided by spatial transcriptomics study. [S43] (B) Percentage of neurons expressing each individual gene and (C) percentage of neurons expressing the most common transcript combinations. Note that genes with low expression levels, such as *OPRM1* and *OPRL1*, as well as *SPP1*, a gene with a high expression level, are not unambiguously assigned to distinct clusters. This is in contrast to our in situ hybridization results, which show *OPRL1* expression in a subpopulation of *TRPV1+OPRM1+* nociceptors, and in a defined, small population of *SPP1+* neurons. In the spatial transcriptomics dataset, *SPP1* appears to be expressed in all clusters compared to the more discrete population seen with in situ hybridization.

Figure S10. Comparison of human DRG in situ hybridization results from this study with spatial transcriptomic data; related to Figure 3 and Discussion.

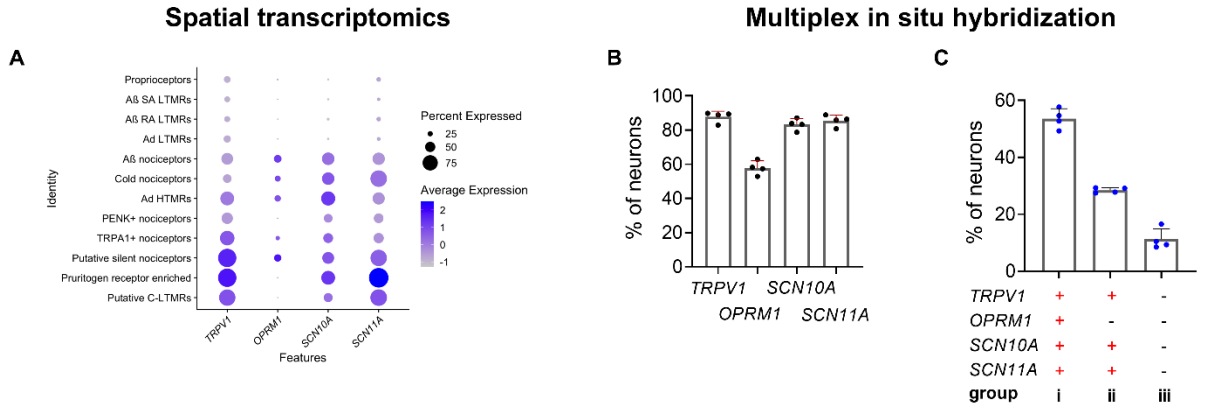

(A) Dot plots demonstrating gene expression in different clusters as provided by spatial transcriptomics study. [S43] (B) Percentage of neurons expressing each individual gene and (C) percentage of neurons expressing the most common transcript combinations. Note that we confirmed the co-expression of *SCN10A* and *SCN11A* in nociceptors (though spatial transcriptomics implies a small percentage of expression in non-nociceptive clusters). Spatial transcriptomics reveal the highest expression level for *SCN11A* in the pruritogen receptor enriched cluster, which aligns with high expression of *SCN11A* in the *TRPV1+OPRM1-* populations (Figure 3). According to spatial transcriptomics data, a small percentage of the pruritogen receptor enriched cluster seem to express *OPRM1*, which is not evident in our results.

Figure S11. Comparison of human DRG in situ hybridization results from this study with spatial transcriptomic data; related to Figure 4 and Discussion.

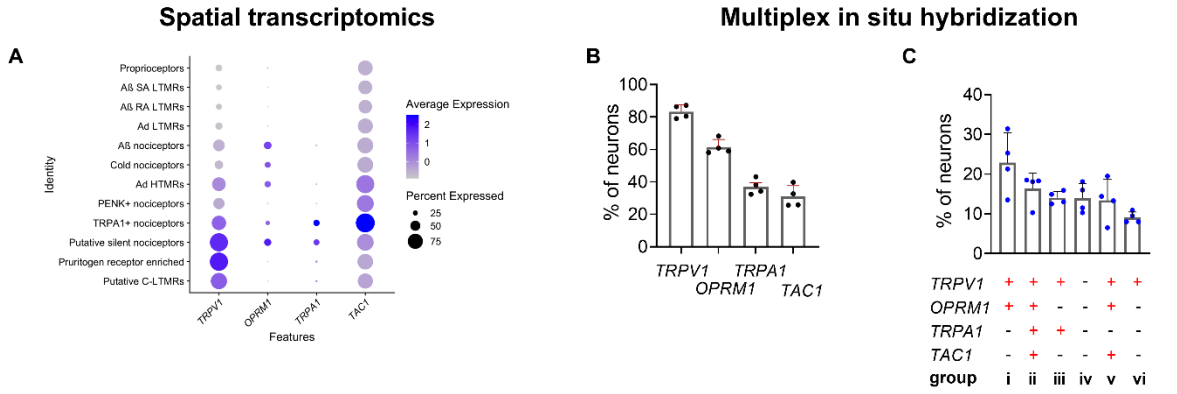

(A) Dot plots demonstrating gene expression in different clusters as provided by spatial transcriptomics study. [S43] (B) Percentage of neurons expressing each individual gene and (C) percentage of neurons expressing the most common transcript combinations. We detected *TRPA1* in more neurons than was detected with spatial transcriptomics. We observed it significantly expressed by a subgroup of *TRPV1+OPRM1-* nociceptors, which potentially corresponds to the pruritogen receptor enriched cluster. In this cluster, *TRPA1* is hardly detected. Another discrepancy is the expression of *TAC1*, which, while focused in the *TRPA1* nociceptor population in (A), is detected in every cluster. This contrasts with the two distinct populations detected with in situ hybridization.

Figure S12. Comparison of human DRG in situ hybridization results from this study with spatial transcriptomic data; related to Figure 7, Figure S6 and Discussion.

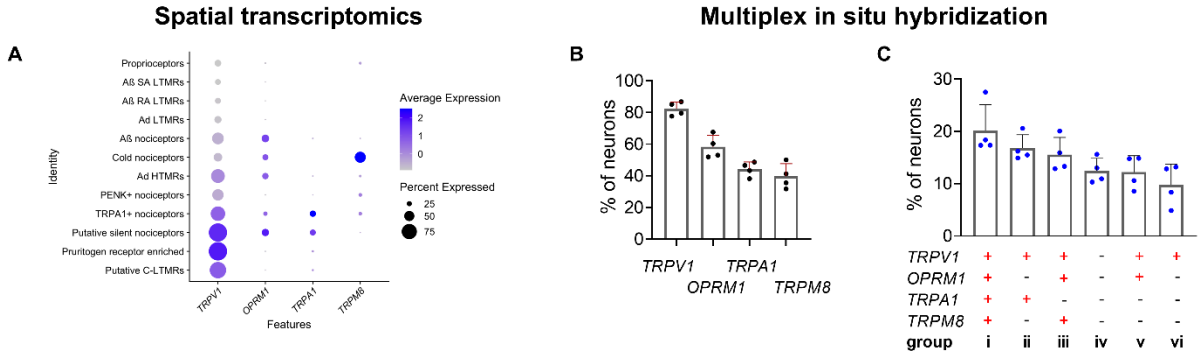

(A) Dot plots demonstrating gene expression in different clusters as provided by spatial transcriptomics (ST) study. [S43] (B) Percentage of neurons expressing each individual gene and (C) percentage of neurons expressing the most common transcript combinations. For *TRPA1*, again we detected, expression in more neurons than was apparent with spatial transcriptomics. We observed *TRPA1* to be significantly expressed by a subgroup of *TRPV1+OPRM1-* nociceptors, which potentially corresponds to the "pruritogen receptor enriched" cluster. In this cluster, *TRPA1* is hardly detected. We classified this cluster as being contained within *TRPV1+OPRM1-* nociceptors. Also, *TRPA1* is expressed in the *TRPV1+OPRM1+* population (C). *TRPM8* was expressed in *TRPV1+OPRM1+* nociceptors, which matches ST results (Figure S6).

Figure S13. Comparison of human DRG in situ hybridization results from this study with spatial transcriptomic data; related to Figure 5 and Discussion.

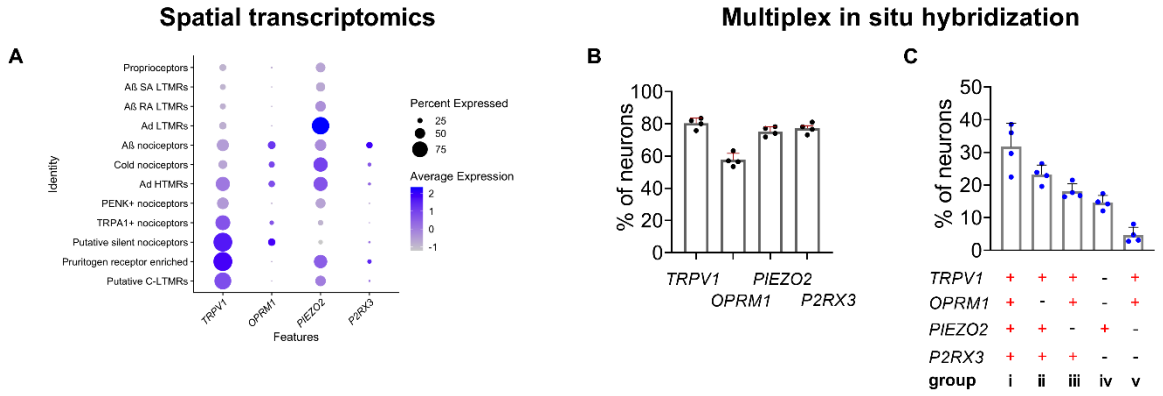

(A) Dot plots demonstrating gene expression in different clusters as provided by spatial transcriptomics (ST) study. [S43] (B) Percentage of neurons expressing each individual gene and (C) percentage of neurons expressing the most common transcript combinations. In contrast to the ST dataset, transcripts for *P2RX3* were detected in an abundance of neurons with in situ hybridization. The result that basically all *TRPV1+OPRM1-* neurons (potentially corresponding to the "pruritogen receptor enriched" cluster) express *PIEZO2* and *P2RX3* (Figure 5) cannot be accurately derived from the ST data.

Figure S14. Comparison of human DRG in situ hybridization results from this study with spatial transcriptomic data; related to Figure 6 and Discussion.

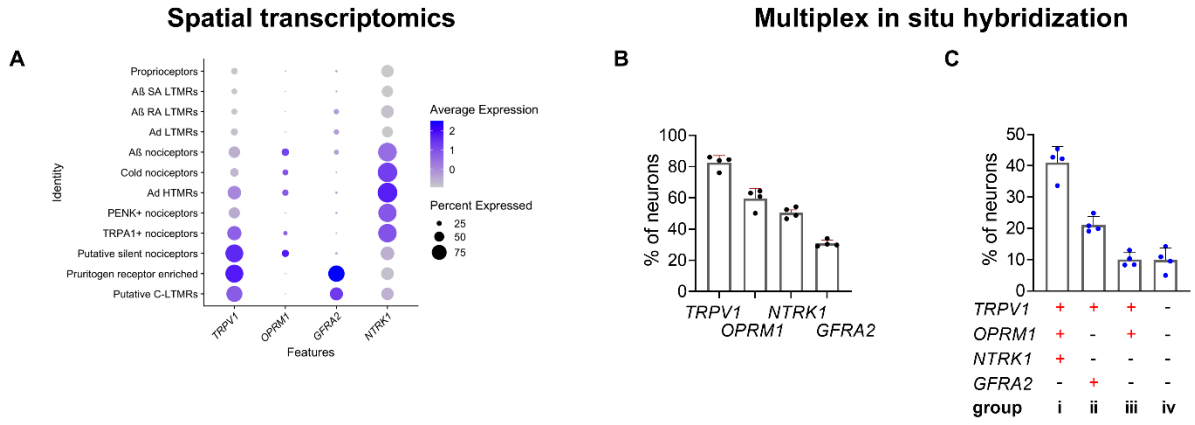

(A) Dot plots demonstrating gene expression in different clusters as provided by spatial transcriptomics (ST) study. [S43] (B) Percentage of neurons expressing each individual gene and (C) percentage of neurons expressing the most common transcript combinations. In the ST dataset, *NTRK1* appears to be expressed in all clusters. This is not supported by the selective expression of *NTRK1* in *TRPV1+OPRM1+* nociceptors. A robust expression of *GFRA2* by *TRPV1+OPRM1-* nociceptors (most likely corresponding to the "pruritogen receptor enriched "cluster) matches results from the ST study presented here.

Figure S15. Comparison of human DRG in situ hybridization results from this study with spatial transcriptomic data; related to Figure 6 and Discussion.

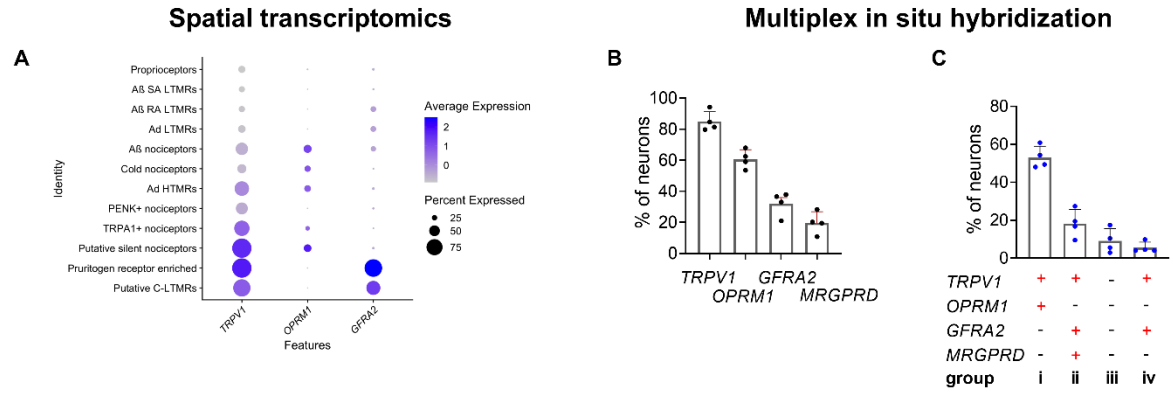

(A) Dot plots demonstrating gene expression in different clusters as provided by spatial transcriptomics (ST) study. [S43] (B) Percentage of neurons expressing each individual gene and (C) percentage of neurons expressing the most common transcript combinations. Note that *MRGPRD*, which is expressed by a major subgroup of *TRPV1+OPRM1-GFRA2+* nociceptors, is not represented in the ST database due to its low expression levels.

Figure S16. UMAP plots derived from spatial transcriptomics study of all gene transcripts investigated in this study, related to Figure 7 and Discussion.

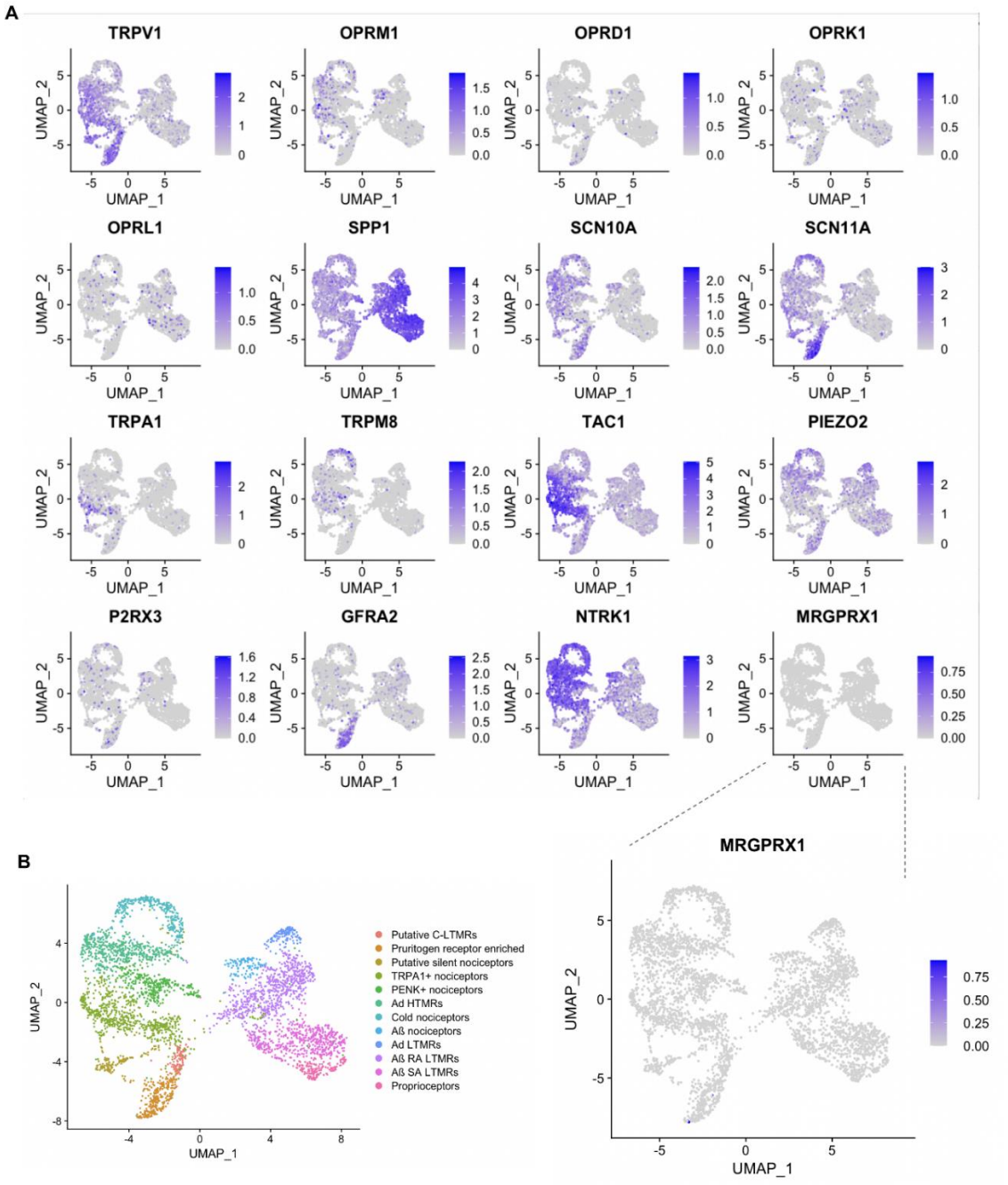

(A) UMAP plots of all genes investigated in this study. Instead of *MRGPRD*, which is not represented in this dataset, we show the highly co-expressed gene *MRGPRX1*. [S44] Note the sparse representation of *MRGPRX1* in the enlarged plot. (B) UMAP plot demonstrating different DRG neuronal clusters. Plots were generated based on online available analyzed data published by Tavares et al. [S3] Note that particularly genes with very low expression levels, such as *OPRD1*, *OPRL1*, and *OPRK1*, and some genes with high expression levels, such as *SPP1*, *TAC1*, and *NTRK1*, appear distributed across all clusters. For *OPRK1* and *SPP1* this could be attributed to nonneuronal gene expression in satellite glial cells or macrophages surrounding DRG neurons, respectively (Figures 1F, S5). [S45,S46,S47]

Supplemental information references

S1. Stacher, G., Steinringer, H., Winklehner, S., Mittelbach, G., and Schneider, C. (1983). Effects of graded oral doses of meptazinol and pentazocine in comparison with placebo on experimentally induced pain in healthy humans. Br J Clin Pharmacol *16*, 149-156. 10.1111/j.1365-2125.1983.tb04979.x.

S2. van der Burght, M., Rasmussen, S.E., Arendt-Nielsen, L., and Bjerring, P. (1994). Morphine does not affect laser induced warmth and pin prick pain thresholds. Acta Anaesthesiol Scand *38*, 161-164. 10.1111/j.1399-6576.1994.tb03859.x.

S3. Gustorff, B., Hoerauf, K.H., Lierz, P., and Kress, H.G. (2003). Comparison of different quantitative sensory testing methods during remifentanil infusion in volunteers. Br J Anaesth *91*, 203-208. 10.1093/bja/aeg161.

S4. Naef, M., Curatolo, M., Petersen-Felix, S., Arendt-Nielsen, L., Zbinden, A., and Brenneisen, R. (2003). The analgesic effect of oral delta-9-tetrahydrocannabinol (THC), morphine, and a THC-morphine combination in healthy subjects under experimental pain conditions. PAIN *105*, 79-88. 10.1016/s0304-3959(03)00163-5.

S5. Angst, M.S., Ramaswamy, B., Davies, M.F., and Maze, M. (2004). Comparative analgesic and mental effects of increasing plasma concentrations of dexmedetomidine and alfentanil in humans. Anesthesiology *101*, 744-752. 10.1097/00000542-200409000-00024.

S6. Cortinez, L.I., Hsu, Y.W., Sum-Ping, S.T., Young, C., Keifer, J.C., Macleod, D., Robertson, K.M., Wright, D.R., Moretti, E.W., and Somma, J. (2004). Dexmedetomidine pharmacodynamics: Part II: Crossover comparison of the analgesic effect of dexmedetomidine and remifentanil in healthy volunteers. Anesthesiology *101*, 1077-1083. 10.1097/00000542-200411000-00006.

S7. Fillingim, R.B., Ness, T.J., Glover, T.L., Campbell, C.M., Hastie, B.A., Price, D.D., and Staud, R. (2005). Morphine responses and experimental pain: sex differences in side effects and cardiovascular responses but not analgesia. J Pain *6*, 116-124. 10.1016/j.jpain.2004.11.005.

S8. Arendt-Nielsen, L., Olesen, A.E., Staahl, C., Menzaghi, F., Kell, S., Wong, G.Y., and Drewes, A.M. (2009). Analgesic efficacy of peripheral kappa-opioid receptor agonist CR665 compared to oxycodone in a multi-modal, multi-tissue experimental human pain model: selective effect on visceral pain. Anesthesiology *111*, 616-624. 10.1097/ALN.0b013e3181af6356.

S9. Eisenberg, E., Midbari, A., Haddad, M., and Pud, D. (2010). Predicting the analgesic effect to oxycodone by 'static' and 'dynamic' quantitative sensory testing in healthy subjects. Pain *151*, 104-109. 10.1016/j.pain.2010.06.025.

S10. Andresen, T., Upton, R.N., Foster, D.J., Christrup, L.L., Arendt-Nielsen, L., and Drewes, A.M. (2011). Pharmacokinetic/pharmacodynamic relationships of transdermal buprenorphine and fentanyl in experimental human pain models. Basic Clin Pharmacol Toxicol *108*, 274-284. 10.1111/j.1742-7843.2010.00649.x.

S11. Angst, M.S., Phillips, N.G., Drover, D.R., Tingle, M., Ray, A., Swan, G.E., Lazzeroni, L.C., and Clark, D.J. (2012). Pain sensitivity and opioid analgesia: a pharmacogenomic twin study. Pain *153*, 1397-1409. 10.1016/j.pain.2012.02.022.

S12. King, C.D., Goodin, B., Glover, T.L., Riley, J.L., Hou, W., Staud, R., and Fillingim, R.B. (2013). Is the pain-reducing effect of opioid medication reliable? A psychophysical study of morphine and pentazocine analgesia. Pain *154*, 476-483. 10.1016/j.pain.2012.12.009.

S13. Olesen, A.E., Brock, C., Sverrisdóttir, E., Larsen, I.M., and Drewes, A.M. (2014). Sensitivity of quantitative sensory models to morphine analgesia in humans. J Pain Res *7*, 717-726. 10.2147/jpr.S73044.

S14. Prosenz, J., and Gustorff, B. (2017). Midazolam as an active placebo in 3 fentanyl-validated nociceptive pain models. Pain *158*, 1264-1271. 10.1097/j.pain.0000000000000910.

S15. Wolff, B.B., Kantor, T.G., Jarvik, M.E., and Laska, E. (1966). Response of experimental pain to analgesic drugs. 1. Morphine, aspirin, and placebo. Clin Pharmacol Ther *7*, 224-238. 10.1002/cpt196672224.

S16. Jarvik, L.F., Simpson, J.H., Guthrie, D., and Liston, E.H. (1981). Morphine, experimental pain, and psychological reactions. Psychopharmacology (Berl) *75*, 124-131. 10.1007/bf00432173.

S17. Posner, J., Telekes, A., Crowley, D., Phillipson, R., and Peck, A.W. (1985). Effects of an opiate on cold-induced pain and the CNS in healthy volunteers. Pain *23*, 73-82. 10.1016/0304-3959(85)90232-5.

S18. Holland, R.L., Harkin, N.E., Coleshaw, S.R., Jones, D.A., Peck, A.W., and Telekes, A. (1987). Dipipanone and nifedipine in cold induced pain; analgesia not due to skin warming. Br J Clin Pharmacol *24*, 823-826. 10.1111/j.1365-2125.1987.tb03253.x.
S19. Cleeland, C.S., Nakamura, Y., Howland, E.W., Morgan, N.R., Edwards, K.R., and Backonja, M. (1996). Effects of oral morphine on cold pressor tolerance time and neuropsychological performance. Neuropsychopharmacology *15*, 252-262. 10.1016/0893-133x(95)00205-r.
S20. Winchester, W.J., Gore, K., Glatt, S., Petit, W., Gardiner, J.C., Conlon, K., Postlethwaite, M., Saintot, P.P., Roberts, S., Gosset, J.R., et al. (2014). Inhibition of TRPM8 channels reduces pain in the cold pressor test in humans. J Pharmacol Exp Ther *351*, 259-269. 10.1124/jpet.114.216010.
S21. Kleine-Borgmann, J., Wilhelmi, J., Kratel, J., Baumann, F., Schmidt, K., Zunhammer, M., and Bingel, U. (2021). Tilidine and dipyrone (metamizole) in cold pressor pain: A pooled analysis of efficacy, tolerability, and safety in healthy volunteers. Clin Transl Sci *14*, 1997-2007. 10.1111/cts.13058.
S22. Watso, J.C., Huang, M., Belval, L.N., Cimino, F.A., 3rd, Jarrard, C.P., Hendrix, J.M., Hinojosa-Laborde, C., and Crandall, C.G. (2022). Low-dose fentanyl reduces pain perception, muscle sympathetic nerve activity responses, and blood pressure responses during the cold pressor test. Am J Physiol Regul Integr Comp Physiol *322*, R64-r76. 10.1152/ajpregu.00218.2021.
S23. Samii, K., Feret, J., Harari, A., and Viars, P. (1979). Selective spinal analgesia. Lancet *1*, 1142.
S24. Wang, J.K., Nauss, L.A., and Thomas, J.E. (1979). Pain relief by intrathecally applied morphine in man. Anesthesiology *50*, 149-151. 10.1097/00000542-197902000-00013.
S25. Baraka, A., Noueihid, R., and Hajj, S. (1981). Intrathecal injection of morphine for obstetric analgesia. Anesthesiology *54*, 136-140. 10.1097/00000542-198102000-00007.
S26. Gray, J.R., Fromme, G.A., Nauss, L.A., Wang, J.K., and Ilstrup, D.M. (1986). Intrathecal morphine for post-thoracotomy pain. Anesth Analg *65*, 873-876.
S27. Abboud, T.K., Dror, A., Mosaad, P., Zhu, J., Mantilla, M., Swart, F., Gangolly, J., Silao, P., Makar, A., Moore, J., and et al. (1988). Mini-dose intrathecal morphine for the relief of post-cesarean section pain: safety, efficacy, and ventilatory responses to carbon dioxide. Anesth Analg *67*, 137-143.
S28. Kirson, L.E., Goldman, J.M., and Slover, R.B. (1989). Low-dose intrathecal morphine for postoperative pain control in patients undergoing transurethral resection of the prostate. Anesthesiology *71*, 192-195. 10.1097/00000542-198908000-00004.
S29. Leighton, B.L., DeSimone, C.A., Norris, M.C., and Ben-David, B. (1989). Intrathecal narcotics for labor revisited: the combination of fentanyl and morphine intrathecally provides rapid onset of profound, prolonged analgesia. Anesth Analg *69*, 122-125.
S30. Cohen, S.E., Cherry, C.M., Holbrook, R.H., Jr., el-Sayed, Y.Y., Gibson, R.N., and Jaffe, R.A. (1993). Intrathecal sufentanil for labor analgesia--sensory changes, side effects, and fetal heart rate changes. Anesth Analg *77*, 1155-1160. 10.1213/00000539-199312000-00013.
S31. D'Angelo, R., Anderson, M.T., Philip, J., and Eisenach, J.C. (1994). Intrathecal sufentanil compared to epidural bupivacaine for labor analgesia. Anesthesiology *80*, 1209-1215. 10.1097/00000542-199406000-00007.
S32. Angel, I.F., Gould, H.J., Jr., and Carey, M.E. (1998). Intrathecal morphine pump as a treatment option in chronic pain of nonmalignant origin. Surg Neurol *49*, 92-98; discussion 98-99. 10.1016/s0090-3019(97)00287-5.
S33. Schuchard, M., Krames, E.S., and Lanning, R. (1998). Intraspinal analgesia for nonmalignant pain: a retrospective analysis for efficacy, safety and feasability in 50 patients. Neuromodulation *1*, 46-56. 10.1111/j.1525-1403.1998.tb00029.x.
S34. Anderson, V.C., and Burchiel, K.J. (1999). A prospective study of long-term intrathecal morphine in the management of chronic nonmalignant pain. Neurosurgery *44*, 289-300; discussion 300-281. 10.1097/00006123-199902000-00026.
S35. Gwirtz, K.H., Young, J.V., Byers, R.S., Alley, C., Levin, K., Walker, S.G., and Stoelting, R.K. (1999). The safety and efficacy of intrathecal opioid analgesia for acute postoperative pain: seven years' experience with 5969 surgical patients at Indiana University Hospital. Anesth Analg *88*, 599-604. 10.1097/00000539-199903000-00026.
S36. Shaladi, A., Saltari, M.R., Piva, B., Crestani, F., Tartari, S., Pinato, P., Micheletto, G., and Dall'Ara, R. (2007). Continuous intrathecal morphine infusion in patients with vertebral fractures due to osteoporosis. Clin J Pain *23*, 511-517. 10.1097/AJP.0b013e31806a23d4.

S37. Zacest, A., Anderson, V.C., and Burchiel, K.J. (2009). The Glass Half Empty or Half Full-How Effective Are Long-Term Intrathecal Opioids in Post-herpetic Neuralgia? A Case Series and Review of the Literature. Neuromodulation *12*, 219-223. 10.1111/j.1525-1403.2009.00218.x.

S38. Fabiano, A.J., Doyle, C., and Plunkett, R.J. (2012). Intrathecal medications in post-herpetic neuralgia. Pain Med *13*, 1088-1090. 10.1111/j.1526-4637.2012.01401.x.

S39. Wang, C., Gu, L., Ruan, Y., Geng, X., Xu, M., Yang, N., Yu, L., Jiang, Y., Zhu, C., Yang, Y., et al. (2019). Facilitation of MrgprD by TRP-A1 promotes neuropathic pain. Faseb j *33*, 1360-1373. 10.1096/fj.201800615RR.

S40. Warwick, C., Cassidy, C., Hachisuka, J., Wright, M.C., Baumbauer, K.M., Adelman, P.C., Lee, K.H., Smith, K.M., Sheahan, T.D., Ross, S.E., and Koerber, H.R. (2021). MrgprdCre lineage neurons mediate optogenetic allodynia through an emergent polysynaptic circuit. Pain *162*, 2120-2131. 10.1097/j.pain.0000000000002227.

S41. Usoskin, D., Furlan, A., Islam, S., Abdo, H., Lönnerberg, P., Lou, D., Hjerling-Leffler, J., Haeggström, J., Kharchenko, O., Kharchenko, P.V., et al. (2015). Unbiased classification of sensory neuron types by large-scale single-cell RNA sequencing. Nat Neurosci *18*, 145-153. 10.1038/nn.3881.

S42. Zylka, M.J., Rice, F.L., and Anderson, D.J. (2005). Topographically distinct epidermal nociceptive circuits revealed by axonal tracers targeted to Mrgprd. Neuron *45*, 17-25. 10.1016/j.neuron.2004.12.015.

S43. Tavares-Ferreira, D., Shiers, S., Ray, P.R., Wangzhou, A., Jeevakumar, V., Sankaranarayanan, I., Cervantes, A.M., Reese, J.C., Chamessian, A., Copits, B.A., et al. (2022). Spatial transcriptomics of dorsal root ganglia identifies molecular signatures of human nociceptors. Sci Transl Med *14*, eabj8186. 10.1126/scitranslmed.abj8186.

S44. Klein, A., Solinski, H.J., Malewicz, N.M., Ieong, H.F., Sypek, E.I., Shimada, S.G., Hartke, T.V., Wooten, M., Wu, G., Dong, X., et al. (2021). Pruriception and neuronal coding in nociceptor subtypes in human and nonhuman primates. Elife *10*. 10.7554/eLife.64506.

S45. O'Brien, E.R., Garvin, M.R., Stewart, D.K., Hinohara, T., Simpson, J.B., Schwartz, S.M., and Giachelli, C.M. (1994). Osteopontin is synthesized by macrophage, smooth muscle, and endothelial cells in primary and restenotic human coronary atherosclerotic plaques. Arterioscler Thromb *14*, 1648-1656. 10.1161/01.atv.14.10.1648.

S46. Szulzewsky, F., Pelz, A., Feng, X., Synowitz, M., Markovic, D., Langmann, T., Holtman, I.R., Wang, X., Eggen, B.J., Boddeke, H.W., et al. (2015). Glioma-associated microglia/macrophages display an expression profile different from M1 and M2 polarization and highly express Gpnmb and Spp1. PLoS One *10*, e0116644. 10.1371/journal.pone.0116644.

S47. Morse, C., Tabib, T., Sembrat, J., Buschur, K.L., Bittar, H.T., Valenzi, E., Jiang, Y., Kass, D.J., Gibson, K., Chen, W., et al. (2019). Proliferating SPP1/MERTK-expressing macrophages in idiopathic pulmonary fibrosis. Eur Respir J *54*. 10.1183/13993003.02441-2018.